ELSEVIER

International Journal of Mass Spectrometry 185/186/187 (1999) 949–959

International Journal of Mass Spectrometry

Gas phase chemistry of pyrene and related cations with molecules and atoms of interstellar interest

Valéry Le Page[a], Yeghis Keheyan[b], Theodore P. Snow[a], Veronica M. Bierbaum[a,*]

[a]*Department of Chemistry and Biochemistry, and Center for Astrophysics and Space Astronomy, University of Colorado, Boulder, CO 80309, USA*
[b]*Istituto di Chimica Nucleare del CNR, Monterotondo Stazione, 00016 Roma, Italy*

Received 9 September 1998; accepted 14 October 1998

Abstract

The chemistry of the pyrene radical cation $C_{16}H_{10}^+$ and its derivatives $C_{16}H_9^+$ and $C_{16}H_{11}^+$ has been investigated in the gas phase using a flowing afterglow-selected ion flow tube. Rate coefficients have been determined for reactions between $C_{16}H_n^+$ (n = 9, 10, 11) and H_2, CO, H_2O, and NH_3 molecules as well as H, O, and N atoms. These studies supplement previous investigations on the smaller benzene and naphthalene cations. It is found that $C_{16}H_{10}^+$ and $C_{16}H_{11}^+$ display consistent, predictable chemistry with reactivities very similar to those of benzene and naphthalene cations. On the other hand, the striking reactivity of $C_{16}H_9^+$ toward atoms, compared to the relative unreactivity of phenylium and naphthylium cations, is believed to result from the triplet nature of this ion in its ground state. Ab initio calculations have been carried out to validate this hypothesis in conjunction with experimental evidence. (Int J Mass Spectrom 185/186/187 (1999) 949–959) © 1999 Elsevier Science B.V.

Keywords: PAH; Ion–molecule reactions; Interstellar chemistry; Flowing afterglow

1. Introduction

Polycyclic aromatic hydrocarbons (PAHs) are thought to be ubiquitous in the interstellar medium (ISM) and they have been proposed, in cationic form, as possible carriers of the diffuse interstellar bands (DIBs) [1] which are visible absorption features in stellar spectra. Their simple composition (both C and H atoms are abundant in environments where DIBs are found) together with the ability of cyclic rings to withstand strong UV flux without undergoing fragmentation support the viability of this hypothesis [2–4].

Although the chemical path leading to the formation of PAHs in the ISM is still unknown and largely open to speculation [5–7], there are even fewer studies about their reactivity in the presence of the other constituents of the diffuse clouds where DIBs mostly appear. The existence of neutral PAHs in the ISM is largely accepted because of their ability to explain certain IR emission features; there are good matches between these emission lines and vibrational transitions in characteristic PAHs [8]. To account for the DIBs, however, PAHs are expected to be in cationic or radical form and the existence of neutrals does not guarantee the presence of cations for their

* Corresponding author.

Dedicated to Professor Michael Bowers on the occasion of his 60th birthday, and in recognition of his seminal contributions to gas phase ion chemistry.

PII S1387-3806(98)14217-3

chemistry will be very different. Thus, it is important to examine the reactivity of $PAHs^+$ with the most common species present in diffuse clouds, namely H_2, H, O, and N, in order to properly evaluate their lifetime in the cloud. Unfortunately there are few studies of the reactivity of organic molecular ions with atoms [9,10]. Most recent studies on $PAHs^+$ have focused on the absorption spectra of cations trapped in inert gas matrices, with a goal of identifying matches with well known DIB wavelengths [11]. These studies are easier for smaller PAH cations where there are few isomers. However, the number of isomers drastically increases for larger $PAHs^+$ and choosing candidates for study becomes a more difficult task.

The purpose of our study of relatively small PAH cations is to give useful guidelines to assess the question of the chemistry of larger PAHs which have more interstellar relevance. These experiments will identify good candidates for IR matrix studies, and possibly, for gas phase spectroscopic studies. Moreover, from these experiments it is found that the reactivity of $PAHs^+$ depend on the size of the molecule (the number of fused rings) and thus one can infer trends which may apply to larger cations.

This study of pyrene cation, as well as protonated and dehydrogenated pyrene cations, extends our previous investigations of benzene and naphthalene cation derivatives [12].

2. Experimental

The experiments were carried out using a flowing afterglow-selected ion flow tube (FA-SIFT) apparatus at the University of Colorado at Boulder. The apparatus has been described elsewhere [13]. Briefly, the technique consists of injecting mass-selected ions in a flow reactor in the presence of neutral reactants and then monitoring the decrease of the reactant ion signal versus time, leading to the determination of the rate coefficient using standard kinetic analysis. The sources and purities of the neutral reactants were described in another paper [14].

In the FA-SIFT experiment $C_{16}H_{10}^+$ is produced by chemical ionization of pyrene with He^+ and also by Penning ionization of pyrene with argon metastables formed in a cold cathode discharge. This latter reaction is not sufficiently exothermic to produce $C_{16}H_9^+$ and therefore the reaction of Ar^+ with pyrene is used to produce this ion. Protonated pyrene is formed by proton transfer from H_3O^+ to pyrene in the source. The N atoms are produced by flowing N_2 through a microwave discharge and the O atoms are derived by subsequent titration with NO. H atoms are formed by passing pure H_2 through the discharge and the atom flow rate is determined using the calibration reaction:

$$C_6H_6^+ + H \rightarrow C_6H_7^+$$
$$\rightarrow C_6H_5^+ + H_2$$

with a known reaction rate coefficient of 2.2×10^{-10} cm^3/s [15,16]. The advantage of using this reaction is that it leads to an accurate measurement of the difference in reactivity of benzene and pyrene cations, and thus allows us to explore the correlation between size and reactivity more accurately than if we used a separate calibration reaction such as $CO_2^+ + H/H_2$ [17]. For reactions of $C_{16}H_{10}^+$ with atoms changes in the transmission of the sampling orifice were examined. In a previous study it was found that the transmission of the sampling orifice decreased (due probably to the formation of an insulating oxide coating) as the duration of the oxygen atom flow increased. This effect, small in the case of H atom reactant, can be drastic for the study of oxygen atoms. To eliminate this effect we measure the ratio of reactant and product ions rather than measuring the decrease of the reactant ion counting rate when flowing atoms. This method, previously applied in our study of reactions between naphthalene cation and atoms, is employed again with only a small change for the reaction between $C_{16}H_{10}^+$ and H atoms. The problem here arises from the difficulty to select cleanly the $^{12}C_{16}H_{10}^+$ cation (mass 202) prior to injection in the reaction flow tube without any contamination by the $^{13}C^{12}C_{15}H_{10}^+$ peak which has the same mass as the product (mass 203, which is about 18% of the mass 202 peak in the source, due to natural abundance of ^{13}C). If k is the rate coefficient of the reaction, [H] the density of hydrogen atoms in the

flow tube, t the reaction time, and $(202/203)_{on/off}$ the counting rate of $^{12}C_{16}H_{10}^+$ over $^{12}C_{16}H_{11}^+$ (with a small contribution of $^{13}C^{12}C_{15}H_{10}^+$ at the same mass) with H_2 flowing, the discharge being on or off, and f_H the transmission factor of the sampling orifice, which depends on H density, we can write, using the standard kinetic law, and assuming no isotope effect on the rate coefficient:

$$(202)_{on} = (202)_{off} \exp(-k[H]t) f_H$$

$$(203)_{on} = [(202)_{off}(1 - \exp(-k[H]t)) + (203)_{off} \exp(-k[H]t)] f_H$$

or, equivalently

$$k[H]t = \ln(1 + R_1 - R_0)$$

where $R_1 = (203/202)_{on}$, and $R_0 = (203/202)_{off}$. Then, the final expression for the rate coefficient is

$$k_{Pyr} = \{\ln(1 + R_1 - R_0)_{[pyr]}/\ln(1 + R_1 - R_0)_{[Bz]}\}k_{Bz}$$

where R_0 and R_1 are the two experimental parameters measured in each case, k_{Pyr} and k_{Bz} the rate coefficients of the reactions between the pyrene cation and H atoms, and the benzene cation and H atoms, respectively. Thus, the procedure is to select $C_{16}H_{10}^+$, which gives $R_{0,pyr}$, and to set a flow of H atoms, leading to the determination of $R_{1,pyr}$. Then, with the same flow we calibrate the H density by selecting $C_6H_6^+$, giving $R_{1,Bz}$, and $R_{0,Bz}$ when the discharge is off. Using this method an average of six runs gave a mean deviation of only about 7% for the determination of the rate coefficient for different hydrogen flows. This procedure was also adapted to assess the question of the reactivity of $C_{16}H_{11}^+$.

3. Results and discussion

3.1. Reactivity of $C_{16}H_{10}^+$

The high stability of the carbon skeleton in this cation makes the opening of the ring very unlikely during reaction with closed shell species. Hydrogen transfer is probably not an efficient process as well because the energy of the C–H bond in $C_{16}H_{10}^+$ is high, around 4.6 eV [18]. Moreover, the low ionization energy of pyrene (7.4 eV [19]) makes charge transfer reactions endothermic for most molecules. Thus, bimolecular channels are not expected to occur during reaction of the pyrene cation with stable molecules. Finally, termolecular association reactions might be inefficient since hydrogen atoms surround the carbon skeleton, providing the ring structure of pyrene is preserved during the ionization process. Indeed, the chemistry of the pyrene cation is much the same as that of benzene or naphthalene cations: the reactivity toward molecules, if any, is very low and a conservative upper limit of 10^{-12} cm^3/s is reported for reactions with H_2, CO, NH_3, and H_2O (see Table 1).

The situation is very different for reaction with transient species like H, O, or N because of the high reactivities of atoms and the absence of activation energies in the case of most radical–radical reactions. Bimolecular channels are probably energetically

Table 1
Rate coefficients and products for the reactions of $C_{16}H_n^+$ (n = 9, 10, 11) with molecules

Ionic reactant	Molecular reactant	Ionic products	Rate coefficient (cm^3/s)[a]
c-$C_{16}H_{11}^+$	H_2	···	No reaction[b]
c-$C_{16}H_{10}^+$	H_2	···	No reaction[b]
	CO, H_2O, NH_3	···	No reaction[c]
c-$C_{16}H_9^+$	H_2		No reaction[b]
	CO	$C_{17}H_9O^+$	4.2×10^{-12} [d]
	H_2O	$C_{16}H_{11}O^+$	4.5×10^{-10} [d]
	NH_3	$C_{16}H_{12}N^+$	3.6×10^{-10} [d]
l-$C_{16}H_9^+$	H_2	···	No reaction[b]
	CO	$C_{17}H_9O^+$	$\sim 2 \times 10^{-14}$ [d]
	H_2O	$C_{16}H_{11}O^+$	$\sim 4 \times 10^{-13}$ [d]
	NH_3	$C_{16}H_{12}N^+$	$\sim 1.5 \times 10^{-11}$ [d]

[a] Rate coefficients are measured at 0.5 torr of helium carrier gas. Estimated total errors: ±30% for cyclic isomers, ±50% otherwise.
[b] No products observed; $k < 5 \times 10^{-13}$ cm^3/s.
[c] No products observed; $k < 1 \times 10^{-12}$ cm^3/s.
[d] Termolecular association reaction.

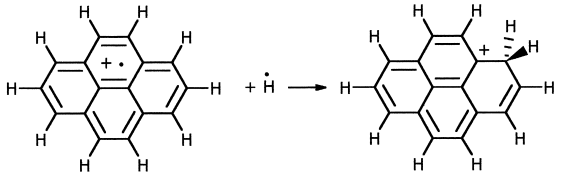

Scheme 1.

available although the major channel in each of the three cases is association with the atomic reactant

$$C_{16}H_{10}^+ + H \rightarrow C_{16}H_{11}^+ \quad 100\%$$

$$C_{16}H_{10}^+ + O \rightarrow C_{16}H_{10}O^+ \quad >95\%$$

$$\rightarrow C_{15}H_{10}^+ + CO \quad <5\%$$

$$C_{16}H_{10}^+ + N \rightarrow C_{16}H_{10}N^+ \quad >95\%$$

$$\rightarrow C_{15}H_9^+ + HCN \quad <5\%$$

The $C_{16}H_{10}^+ + H$ reaction is the most simple case. The heat of formation of $C_{16}H_9^+$ has been recently estimated by Ling et al. to be ~284 kcal/mol at 0 K [18]. Thus, the reaction $C_{16}H_{10}^+ + H \rightarrow C_{16}H_9^+ + H_2$ is endothermic and the only available channel for reaction is association with H (see Scheme 1).

The H abstraction channel appears to have a large exothermicity only in the benzene case due to the relatively small energy needed to break a C–H bond [20]. For larger $PAHs^+$ this bond energy seems to approach the value of the energy necessary to break a C–H bond in a neutral PAH (~4.8 eV), a relatively high value which makes the H_2 formation channel endothermic. In the case of reactions with O and N the channels forming CO and HCN, respectively, are much less efficient than in the cases of $C_6H_6^+$ and $C_{10}H_8^+$. A likely explanation lies in the number of degrees of freedom available to the intermediate complex formed during the association between the cation and the atom; these larger complexes store the excess energy more readily. The lifetime of the complex will increase from benzene to pyrene thus favoring the occurrence of a stabilizing collision with the buffer gas which removes the excess energy of the intermediate. Recently, Sommer and Roth, investigating the $C_{60} + O$ reaction in a shock tube near 2000 K,

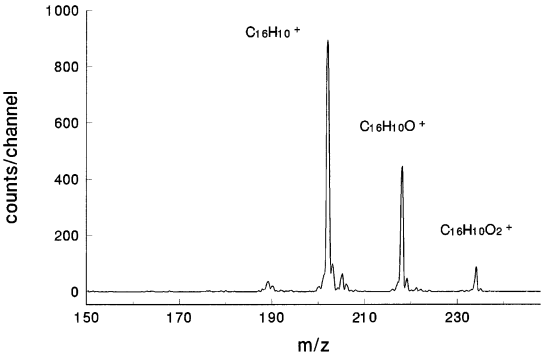

Fig. 1. A mass spectrum of the products of the reaction between $C_{16}H_{10}^+$ and O atoms. $C_{16}H_{10}O_2^+$ is a secondary product arising from reaction of $C_{16}H_{10}O^+$, which is the only detectable primary product.

have seen formation of CO which was detected as the main oxidation product [21]. The formation of an epoxide structure $C_{60}O$ was regarded as a possible second reaction channel. The presence of the fullerene $C_{60}O_n$ adducts (up to $n = 5$) has also been reported by Wood et al. in extracts prepared from soot produced by using resistive heating of graphite [22]. Spectroscopic studies of Creegan et al. strongly support an epoxide structure for the $C_{60}O$ complex [23]. In our experiments of benzene, naphthalene, and pyrene cations we note that the major product arises from C or CH abstraction in the benzene case (formation of CO and HCN, respectively), from both abstraction and association for naphthalene and, finally, essentially only from addition for reaction between pyrene cation and N or O atoms (see Fig. 1). Table 2 presents the rate coefficients of reactions between $C_{16}H_{10}^+$ and atoms together with the corresponding results for $C_{16}H_9^+$ and $C_{16}H_{11}^+$. The low reactivity of $C_{16}H_{10}^+$ toward N atoms in the reaction

$$C_{16}H_{10}^+(S = 1/2) + N(S=3/2) \rightarrow C_{16}H_{10}N^+(S=0)$$

$$k = 1.5\times10^{-12}\ cm^3/s$$

is understood as a consequence of the violation of the Wigner-Witmer rule on spin conservation [24].

Table 2
Rate coefficients and products for the reactions of $C_{16}H_n^+$ (n = 9, 10, 11) with atoms

Ionic reactant	Atomic reactant	Ionic products (branching ratio)	Rate coefficient (cm^3/s)[a]
$C_{16}H_{11}^+$	H	c-$C_{16}H_{12}^+$	$\sim 3 \times 10^{-12}$
	O	No reaction[b]	
	N	No reaction[c]	
$C_{16}H_{10}^+$	H	$C_{16}H_{11}^+$ (1.0)	1.4×10^{-10}
	O	$C_{16}H_{10}O^+$ (>0.95)	9.5×10^{-11}
	N	$C_{16}H_{10}N^+$ (>0.95)	1.5×10^{-12}
$C_{16}H_9^+$	H	$C_{16}H_{10}^+$ (1.0)	$\sim 1.6 \times 10^{-10}$ [d]
	O	$C_{16}H_9O^+$ (~0.5)	$\sim 2 \times 10^{-10}$ [d]
		$C_{15}H_9^+$ (~0.5)	
	N	$C_{16}H_9N^+$ (>0.8)	$\sim 3 \times 10^{-11}$ [d]

[a] Represents reactivity of cyclic reactant ion, unless otherwise specified. Estimated total errors: ±30% for reactions between $C_{16}H_{10}^+$ and H atoms and O atoms; ±50% otherwise. This table extends previous measurements obtained on the pyrene system [38].

[b] $k < 3 \times 10^{-11}$ cm^3/s.

[c] $k < 5 \times 10^{-12}$ cm^3/s.

[d] Reactivity due to both cyclic and acyclic reactant ions. Although it is not rigorous to assign a value for a rate constant involving two isomers, it is useful as an estimation of the reactivity. Furthermore, as in the doubly dehydrogenated naphthalene $C_{10}H_6^+$ case, no evidence was found for a different reactivity of the isomers.

3.2. Reactivity of $C_{16}H_9^+$

As in the case of $C_{10}H_7^+$ or $C_6H_5^+$ the total signal of dehydrogenated pyrene is composed of two isomers with one being more reactive than the other (except toward H_2 which is essentially unreactive with $C_{16}H_9^+$). It is likely that one isomer retains the cyclic structure while the second isomer (possibly consisting of several forms) has an altered carbon skeleton with a broken CC bond. Following previous studies on the benzene [25] and naphthalene systems [14] we assign the cyclic form to the reactive isomer. Fortunately there is usually one order of magnitude difference between the two rate coefficients and thus it is possible to set the neutral reactant flow in such a way that only one isomer is primarily reacting. For instance, experiments at a very low density of neutral allow us to extract the larger rate coefficient (the decrease of the other isomer is only a few percent);

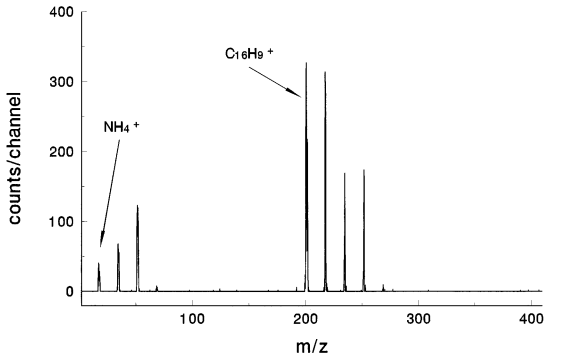

Fig. 2. Mass spectrum of the reaction $C_{16}H_9^+ + NH_3$ at high density of NH_3 (about 4×10^{13} cm^{-3}). The primary product $C_{16}H_{12}N^+$ undergoes further addition of ammonia as well as production of NH_4^+, which in turn gives $NH_4^+(NH_3)_n$.

working at a higher flow allows us to extract the smaller rate coefficient since at this flow the more reactive isomer has been completely converted to product (see Fig. 2). Fig. 3 shows a typical extraction of the larger rate coefficient in the case of the reaction $C_{16}H_9^+ + NH_3$. $C_{16}H_9^+$ is produced using the reaction between Ar^+ and pyrene in the source which forms both $C_{16}H_9^+$ and $C_{16}H_{10}^+$. The $C_{16}H_9^+$ cation is then selected using a quadrupole filter and injected into the reaction flow tube. The major drawback of this procedure for relatively high masses such as pyrene (m/z = 202 amu) is the selection of both pyrenium and pyrene ion. Clean selection of the pyrenium cation would be possible only at higher resolution, and this will lower the quadrupole transmission by such an extent that quantitative analysis is not feasible. However, the pyrene peak at mass 202 will not affect the counting rate of the pyrenium cation at mass 201 because the pyrene cation appears to be unreactive with all the molecules in this study. Another problem comes from the small contribution of the more reactive isomer in the overall peak. For these reasons the extraction of the rate coefficient is made by monitoring the product peak versus the reaction time and, in the case of the reaction $C_{16}H_9^+ + NH_3$, at a sufficiently low reactant density to ensure that secondary reactions remain negligible. From a fitting of a single exponential to these data it is possible to extract the rate coefficient and also the proportion of

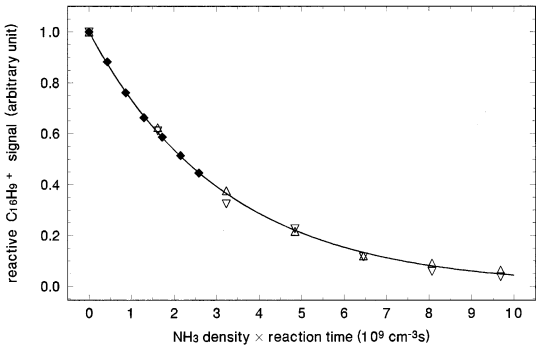

Fig. 3. An example of extraction of the rate coefficient of the reaction between *c*-$C_{16}H_9^+$ and NH_3. This experiment is carried out at low NH_3 density in order to avoid both secondary reactions ($C_{16}H_{12}N^+$ is still the major product with a branching ratio over 0.95) and reaction of the less reactive isomer. The fitted curve is calculated using only the diamond symbols from an experiment carried out at a low density of 5×10^{11} cm^{-3}. These measurements are in very good agreement with two other experiments (triangles up and down) carried out at a density of 2×10^{12} cm^{-3}, showing evidence for reaction of only one of the two isomers. At the lowest density the decrease of the $C_{16}H_9^+$ peak is expected to be primarily (95%) due to the reactive isomer. Thus, the effect of the less reactive isomer has not been taken into account in the calculation of the rate coefficient.

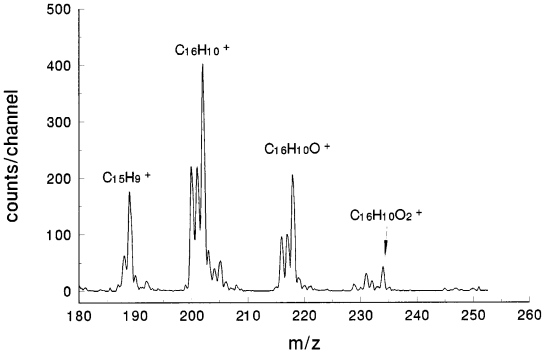

Fig. 4. Injection of $C_{16}H_8^+$, $C_{16}H_9^+$, and $C_{16}H_{10}^+$ and reaction with O atoms. One can see that no product is formed at mass 233 ($C_{16}H_9O_2^+$), consistent with the expected singlet state of $C_{16}H_9O^+$ and its lack of reactivity with O. The $C_{15}H_9^+$ ion is formed from the reaction $C_{16}H_9^+ + O$, with release of a CO molecule. The reactions are similar to those seen with naphthalene cation with a preference for association rather than bimolecular reactions.

the reactive isomer in the total signal. Our independent finding that the reactive isomer accounts for ~30% in each reaction validates this approach (the proportion of reactive isomers in reactions with CO, H_2O, and NH_3 was found to be 30%, 28%, and 32%, respectively). For all the reactions of $C_{16}H_9^+$ with molecules the only observed primary channel is association with the neutral. This is partly due to the exceptional stability of the carbon skeleton of pyrene which is composed of fused benzene rings. Table 1 summarizes the rate coefficients for all reactions studied of pyrene cations with molecules. The reactivity of $C_{16}H_9^+$ is much lower than the reactivity of either phenylium or naphthylium cations. The unreactivity of $C_{16}H_9^+$ toward molecular hydrogen is surprising considering that $C_6H_5^+$ and $C_{10}H_7^+$ display a similar rate coefficient of about 5×10^{-11} cm^3/s for this reaction.

Table 2 summarizes the chemistry of reactions between cations and atoms. In this case the pyrenium ion $C_{16}H_9^+$ appears to be much more reactive with atoms than are the smaller naphthylium and phenylium cations. This behavior of $C_{16}H_9^+$, facile reaction with atoms and low reactivity toward molecules, is typical of radical cations like $C_{16}H_{10}^+$. Indeed, we believe that $C_{16}H_9^+$ is a triplet ground state ion and below we present experimental and theoretical evidence which supports this assumption.

We base our discussion on a comparison between the pyrene cation family (including dehydrogenated pyrene) and the naphthalene cation family. We have seen that the naphthyl cation $C_{10}H_7^+$ was not reactive toward O atoms in agreement with the singlet nature of this ion (from ab initio calculations) while $C_{10}H_8^+$ adds as many as four oxygen atoms in consecutive steps. When adding an oxygen atom the naphthalene radical cation retains its radical character and thus further reactions with oxygen can occur through fast and efficient radical–radical reactions. Fig. 4 shows the overall reactivity of the pyrene family. In Fig. 4 one can see the oxygen additions proceed from $C_{16}H_{10}^+$ up to $C_{16}H_{10}O_2^+$ which is similar to the reaction of the naphthalene cation. If $C_{16}H_9^+$ is a triplet ion the reaction between $C_{16}H_9^+(S = 1)$ and $O(S = 1)$ is spin-allowed, giving $C_{16}H_9O^+$ at mass 217, probably in a conventional singlet ground state. The absence of further addition between $C_{16}H_9O^+$ and O with an expected product at mass 233 amu can

Table 3
Ab initio calculations of singlet–triplet splitting of cyclic hydrocarbons

	Singlet–triplet splitting (kcal/mol)[a]			
Level of calculation[b]	$C_5H_5^+$	$C_6H_5^+$ ($^3B_1-{}^1A_1$)	$C_{10}H_7^+$ [c] ($^3A''-{}^1A'$)	$C_{16}H_9^+$ [d] ($^3A'-{}^1A'$)
ROHF/6-31G*	−35.0	−1.9	−14.7	−26.4
MP2/6-31G*	−25.6	24.4	14.6	
MP3/6-31G*	−27.2	15.2	3.3	
ROMP2/6-31G*	−27.1	21.1	−1.8	−15.3
Exp ground state	Triplet[e]	Singlet[f]	Singlet[f]	Triplet[f]

[a] Energy (triplet)–energy (singlet).
[b] All energies are computed using the corresponding optimized geometry (singlet or triplet) at the ROHF level using the 6-31G* basis set, except for $C_5H_5^+$ where both calculations are done with the triplet optimized geometry. Changes in ZPE are not included.
[c] Calculations are given for the 2-dehydro naphthalene cation (missing hydrogen on a carbon at the outermost position with respect to the central CC bond). Results are essentially the same for the 1-dehydro naphthalene cation (loss of an H atom near the central CC bond) at the ROHF, MP2, and MP3 level (ROMP2 calculations were not carried out for the 1-dehydro cation). No spin contaminations were found in these calculations.
[d] Calculations done for only one dehydrogenated isomer. Computations at the MP2 and MP3 levels were not attempted.
[e] [31].
[f] Inferred from the specific reactivities with atoms and molecules.

be understood as observance of the spin conservation rule because the reaction between the singlet $C_{16}H_9O^+$ and an oxygen triplet is not allowed to give the doublet $C_{16}H_9O_2^+$. The opposite reactivities of $C_{16}H_9^+$ and $C_{16}H_9O^+$ is thus probably due to the different states of these two ions. Moreover, the same argument applies to the reaction $C_{16}H_9^+ + N$ which appears to be more than one order of magnitude faster than the corresponding spin-forbidden reaction $C_{16}H_{10}^+ + N$. This difference can again be explained if we consider that $C_{16}H_9^+$ is a triplet ground state cation, which makes the reaction allowed.

We have performed ab initio calculations using the commercial Gaussian 94 program [26] for the purpose of evaluating the singlet–triplet splitting of $C_{16}H_9^+$. From an initial geometry from Toussaint et al. [27], and after a first geometry optimization using the semiempirical method PM3 [28], we have performed a geometry optimization at the ROHF/6-31G* level for each state followed by a single point calculation at the ROMP2/6-31G* level. The singlet–triplet splitting, neglecting the zero point energy of each ion [ΔZPE $<$ 0.1 kcal/mol between $C_{16}H_9^+(S)$ and $C_{16}H_9^+(T)$ from a PM3 calculation], was found to favor the triplet over the singlet state by 15.3 kcal/mol.

Finally, we note that $C_{16}H_9^+$, with 14 π electrons, could be a triplet ground state ion according to Hückel's theory, together with Hund's rule, if we view this molecule as being split into an annulene molecule (a monocyclic conjugated system with 14 carbons for which the $4n + 2$ Hückel's rule is strictly applicable [29]) bearing 12 π electrons and 2 central carbons regarded as a perturbation of the annulene ring [30]. With 12 π electrons the annulene ring is a good triplet candidate as is, e.g. the cyclopentadienyl cation with 4 π electrons which has been reported experimentally to be a triplet ground state cation [31].

In order to validate this result we have performed calculations on the phenyl cation singlet–triplet splitting at the same level of theory. A splitting of 21 kcal/mol is found in reasonable agreement with the recent high-level ab initio calculations of Radom et al. [32] where the triplet was found to be 24.7 kcal/mol above the singlet. This calculation is also in good agreement with the work of Hrušák et al. [33] who estimated the same singlet–triplet gap to be about 18 kcal/mol. Table 3 summarizes our results on various cyclic hydrocarbon cations. From Table 3 it is clear that the restricted open-shell Hartree-Fock (ROHF) level is not sufficiently accurate to determine which state is most likely to be the ground state; however, MP2, MP3, and ROMP2 calculations are consistently

closer in their predictions, which agree well with the experiment of Saunders et al. [31] on the nature of the ground state of $C_5H_5^+$ and with our own experimental assignment of the ground state of $C_6H_5^+$, $C_{10}H_7^+$, and $C_{16}H_9^+$ in view of their specific chemistry with atoms and molecules.

We can further link the value of Δ_{TS} of $C_{16}H_9^+$ with the recent experimental work of Lifshitz and co-workers on the photodissociation of pyrene cation [18] using the time-resolved photoionization mass spectrometry technique (TPIMS). In their study the pyrene molecule was ionized and excited using a photon of known wavelength and then trapped in a Paul-type cylindrical ion trap. Next, the ions were ejected and mass analyzed in a conventional mass spectrometer after a variable delay time. From the analysis of the dissociation rate of the pyrene cation versus the energy of the incident photons using a Rice-Ramsperger-Kassel-Marcus (RRKM) fit the authors were able to extract the activation energy involved in each dissociation process, basically ejection of a H_2 molecule or consecutive loss of two H atoms. This was the first study able to clearly differentiate the H_2 loss reaction from the two consecutive $H^{\bullet}$ losses in pyrene. With their experimental data Lifshitz and co-workers determined the enthalpy of formation of $C_{16}H_8^+$ to be 327.2 kcal/mol at 0 K assuming that the two consecutive $H^{\bullet}$ loss processes have no reverse activation energy (the curves were well-fitted using a loose transition state which indicates a simple bond cleavage). However, a value lower or equal to 311 kcal/mol was deduced from the direct H_2 loss process (this latter mechanism was fitted using a tight transition state, indicating a probable reverse activation energy, and thus only an upper limit was determined for $\Delta H_f^0(C_{16}H_8^+)$. No explanation was found to elucidate the problem raised by these contradictory results. However, if we assume $C_{16}H_9^+$ to be a triplet ground state cation, it is clear that there must be some activation energy in the reverse $C_{16}H_9^+ + H$ reaction; in the $^3A'$ state there is a lone electron pair on the carbon which lacks a hydrogen atom and, consequently, the potential energy surface for the H addition reaction might be repulsive due to the three-electron interaction when a H atom approaches the reactive site. Following Klippenstein [34] in his study of the dissociation of $C_6H_6^+$ whose results suggest that the $C_6H_5^+$ product is in the singlet state, we might equate the activation energy with our estimated singlet–triplet splitting. When estimating the enthalpy of formation of $C_{16}H_8^+$ one must take into account the additional energy carried by the ejected hydrogen atom because if there is an activation energy in the $C_{16}H_9^+ + H$ reaction, the ejected H atom in the reverse photodissociation process carries almost all of this energy. This leads to a new value of 311.9 kcal/mol for the $C_{16}H_8^+$ cation in better agreement with the expected value $\leq$311 kcal/mol. Furthermore, using the SIFT apparatus, we have found that there are no reactions between $C_{16}H_8^+$ and H_2 and D_2 which indicates the existence of an activation energy also in these processes. In summary, the results of Lifshitz and co-workers argue in favor of a Δ_{TS} for $C_{16}H_9^+$ greater or equal to 16.2 kcal/mol, in reasonable agreement with our finding of Δ_{TS} = 15.3 kcal/mol considering the experimental uncertainties of both the TPIMS experiments and the ab initio calculation.

Having confidence in the result of our calculation of Δ_{TS}, it is now possible to understand why $C_{16}H_9^+$ is reactive toward NH_3, CO, and H_2O while it is not reactive with H_2. A lack of reactivity is not expected if $C_{16}H_9^+$ were a singlet ground state ion because $C_6H_5^+$ and $C_{10}H_7^+$, both singlet, react efficiently with H_2. We can rationalize this behavior on the basis of frontier orbital theory in selecting the interactions between the molecular orbitals (MO) of both reactants which are most likely to play a key role during the reaction [35,36]. Indeed, if we consider the $C_{16}H_9^+$ cation in a triplet $^3A'$ state (see Fig. 5) we have 14 electrons on the π system with two of them being unpaired on the two highest singly occupied molecular orbitals (SOMO) and, also, a nonbonding σ pair on the carbon atom where the hydrogen is missing. The situation is different if we compare it to $C_{10}H_7^+$ or $C_6H_5^+$ where there is a complete filling of the π bonding orbitals and an empty σ nonbonding orbital on the carbon where there is no hydrogen atom. There is probably a strong interaction between this empty MO and the σ-H_2 MO in the $C_{10}H_7^+ + H_2$ and the

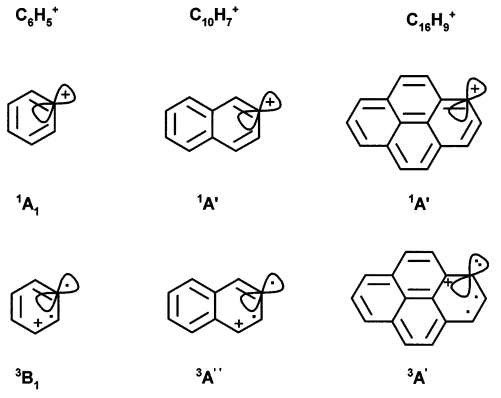

Fig. 5. States involved in the calculation of the singlet–triplet splitting for dehydrogenated cyclic hydrocarbon cations.

$C_6H_5^+ + H_2$ cases, leading to the formation of the $C_{10}H_9^+$ and $C_6H_7^+$ products via nucleophilic addition. In the case of $C_{16}H_9^+$ this is no longer possible because this MO is now filled with the lone pair and the interaction between the σ-H_2 and this nonbonding MO is a 4 electron interaction which is repulsive. Thus, the $C_{16}H_9^+ + H_2$ reaction cannot proceed.

However, for NH_3, H_2O, and possibly CO there is an interaction between the π SOMOs on $C_{16}H_9^+$ (triplet) and a lone pair on the neutral molecule with the appropriate symmetry. Consequently, the reaction between triplet-$C_{16}H_9^+$ and NH_3, H_2O, CO could be initiated through this π interaction, something which is not possible in the H_2 case.

Fig. 6 shows the corresponding interactions in the H_2 and NH_3 case. The lone pair on the carbon where a H is missing does not interact with the filled σ orbital of H_2. For NH_3 the $1e_x$ and $1e_y$ orbitals can interact with the two singly occupied π orbitals of $C_{16}H_9^+$ (or, at least, one of them, the other being perpendicular and thus nonbonding). This overall bonding interaction could explain why the reaction proceeds. Subsequently the molecular ion will undergo a transition from triplet to singlet (the ground state for the $C_{16}H_9NH_3^+$ product from calculation at the ROMP2/6-31G*//ROHF/6-31G* level) with formation of a σ-CN bond. The picture in the H_2O and CO cases is essentially the same with the $1b_1$ and $1b_2$ orbitals of H_2O and the $1\pi_x$ and $1\pi_y$ orbitals of CO being able to react with the two π SOMOs of $C_{16}H_9^+$.

3.3. Reactivity of $C_{16}H_{11}^+$

In the ISM the abundance of H or H_2 over other atomic or molecular species and the fast hydrogenation rate of $C_{16}H_9^+$ and $C_{16}H_{10}^+$ suggests that protonated pyrene $C_{16}H_{11}^+$ is the terminal ionic species in diffuse clouds. Thus, it is important to test the reactivity of this ion with H_2, H, O, and N.

No evidence for reaction was found for H_2, O, and N. The only detectable reaction occurs with H atoms with the product being $C_{16}H_{12}^+$. The results are reported in Table 2. The rate coefficient for this reaction ($k \sim 3 \times 10^{-12}$ cm^3/s) is very close to the corresponding ones for protonated benzene and protonated naphthalene (4×10^{-12} cm^3/s for both of these ions). The implications of these results will be discussed in a forthcoming paper [37]. However, we can note briefly that the lifetime of $C_{16}H_{11}^+$ with respect to H addition (about 10^3 years) is much greater than the lifetime due to electron recombination (about a few decades). Thus, one of the main depletion mechanisms of $C_{16}H_{11}^+$ should be electron recombination. Consequently, the nature of the products of the electron recombination process appears to be a central concern in the PAH hypothesis as well as the effectiveness of photodissociative channels; a crucial point is the fraction of the electronic recombination (and the UV absorption) which is truly dissociative [38].

4. Conclusion

The fast association reactions of dehydrogenated pyrene cation and pyrene cation with H atoms, together with the fact that the terminal ion $C_{16}H_{11}^+$ is almost unreactive in the presence of H_2, H, N, and O, confirms our previous conclusions in our benzene and naphthalene studies; namely the protonated PAHs, or closely related species, seem to rank among the best candidates for IR matrix studies devoted to PAHs$^+$ in the ISM. The general chemistry of pyrene is found to be very close to that of benzene or naphthalene except for the dehydrogenated pyrene cation which displays a peculiar chemistry which is understood as a sign of a triplet ground state for this cation. Thus, the com-

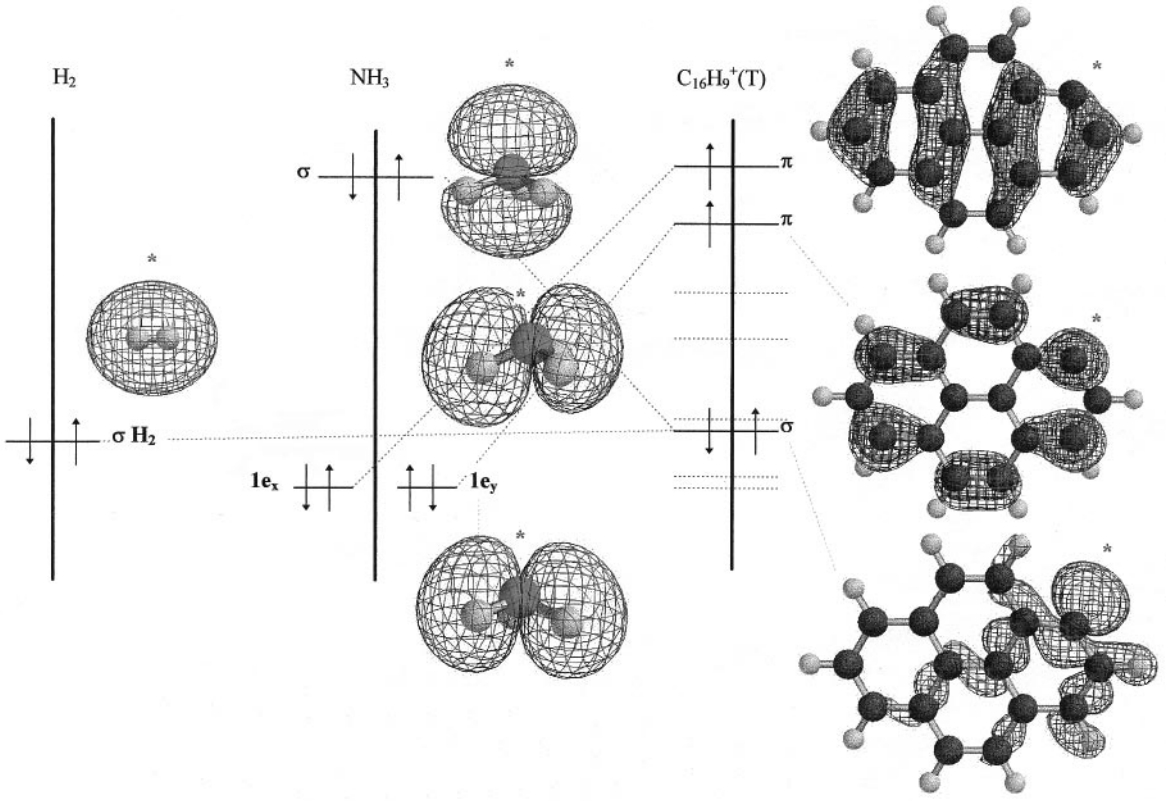

Fig. 6. Correlation diagram for the $C_{16}H_9^+$ (T) + H_2, NH_3 reactions. Electron densities are calculated at the UHF/6-31G* level with molecular geometries optimized at the ROHF/6-31G* level. Energy levels are calculated at the ROMP2/6-31G*//ROHF/6-31G* level.

parison between benzene, naphthalene and pyrene provides guidelines to assess the reactivity of larger PAH cations.

Acknowledgements

This research was sponsored by the National Aeronautics and Space Administration. The computational studies were supported by the National Science Foundation (CHE-9734867).

References

[1] G.P. Van der Zwet, L.J. Allamandola, Astron. Astroph. 146 (1985) 76–80; A. Léger, L. d'Hendecourt, ibid. 146 (1985) 81–85; M.K. Crawford, A.G.G.M. Tielens, L.J. Allamandola, Astrophys. J. 293 (1985) L45–48.
[2] H.W. Jochims, E. Rühl, H. Baugmartel, S. Tobita, S. Leach, Astrophys. J. 420 (1994) 307–317.
[3] S.J. Pachuta, H.I. Kenttämaa, T.M. Sack, R.L. Cerny, K.B. Tomer, M.L. Gross, R.R. Pachuta, R.G. Cooks, J. Am. Chem. Soc. 110 (1988) 657–665.
[4] T.P. Snow, in From Stardust to Planetesimals, Y.J. Pendleton, A.G.G.M. Tielens (Eds.), ASP Conference Series Vol. 122, San Francisco, 1997, pp. 147–157.
[5] M. Frenklach, E. Feigelson, in From Stardust to Planetesimals, Y.J. Pendleton, A.G.G.M. Tielens (Eds.), ASP Conference Series Vol. 122, San Francisco, 1997, pp. 107–116.
[6] P. Marty, P. de Parseval, A. Klotz, B. Chaudret, G. Serra, P. Boissel, Chem. Phys. Lett. 256 (1996) 669–674.
[7] D.K. Bohme, Chem. Rev. 92 (1992) 1487–1508.
[8] L.J. Allamandola, A.G.G.M. Tielens, J.R. Barker, Astroph. J. Suppl. Ser. 71 (1989) 733–775.
[9] H. Becker, G. Javahery, S. Petrie, J. Am. Chem. Soc. 15 (1993) 11636–11637.
[10] M. Sablier, C. Rolando, Mass Spectrom. Rev. 12 (1993) 285–312.
[11] C. Joblin, F. Salama, L.J. Allamandola, in The Diffuse

Interstellar Bands, A.G.G.M. Tielens, T.P. Snow (Eds.), Kluwer, Dordrecht, The Netherlands, 1995, pp. 157–163.
[12] V. Le Page, Y. Keheyan, V.M. Bierbaum, T.P. Snow, J. Am. Chem. Soc. 119 (1997) 8373–8374.
[13] J.M. Van Doren, S.E. Barlow, C.H. DePuy, V.M. Bierbaum, Int. J. Mass Spectrom. Ion Processes 109 (1991) 305–325.
[14] V. Le Page, Y. Keheyan, T.P. Snow, V.M. Bierbaum, J. Am. Chem. Soc., in press.
[15] S. Petrie, G. Javahery, D.K. Bohme, J. Am. Chem. Soc. 114 (1992) 9205–9206.
[16] G.B. Scott, D.A. Fairley, C.G. Freeman, M.J. McEwan, N.G. Adams, L.M. Babcock, J. Phys. Chem. A 101 (1997) 4973–4978.
[17] P. Tosi, S. Ianotta, D. Bassi, H. Villinger, W. Dobler, W. Lindinger, J. Chem. Phys. 80 (1984) 1905–1906.
[18] Y. Ling, Y. Gotkis, C. Lifshitz, Eur. Mass Spectrom. 1 (1995) 41–49.
[19] S.G. Lias, J.E. Bartmess, J.F. Liebman, J.L. Holmes, R.D. Levin, W.G. Mallard, J. Phys. Chem. Ref. Data 17 Suppl 1 (1988).
[20] H.J. Neusser, J. Phys. Chem. 93 (1989) 3897–3907.
[21] T. Sommer, P.J. Roth, J. Phys. Chem. 101 (1997) 6238–6242.
[22] J.M. Wood, B. Kahr, S.H. Hoke II, L. Dejarme, G. Cooks, D. Ben-Amotz, J. Am. Chem. Soc. 113 (1991) 5907–5908.
[23] K.M. Creegan, J.L. Robbins, J.M. Millar, R.D. Sherwood, P.J. Tindall, D.M. Cox, A.B. Smith, J.P. McCauley, D.R. Jones, R.T. Gallagher, J. Am. Chem. Soc. 114 (1992) 1103–1105.
[24] R.G. Pearson, Symmetry Rules for Chemical Reactions, Wiley, New York, 1976.
[25] P. Ausloos, S.L. Lias, T.J. Buckley, E.E. Rogers, Int. J. Mass Spectrom. Ion Processes 92 (1989) 65–77.
[26] M.J. Frish, G.W. Trucks, H.B. Schlegel, P.M.W. Gill, B.G. Johnson, M.A. Robb, J.R. Cheeseman, T.A. Keith, G.A. Petersson, J.A. Montgomery, K. Raghavachary, M.A. Al-Laham, V.G. Zakrzewski, J.V. Ortiz, J.B. Foresman, J. Cioslowski, B.B. Stefanov, A. Nanayakkara, M. Challacombe, C.Y. Peng, P.Y. Ayala, W. Chen, M.W. Wong, J.L. Andres, E.S. Replogle, R. Gomperts, R.L. Martin, D.J. Fox, J.S. Binkley, D.J. Defrees, J. Baker, J.P. Stewart, M. Head-Gordon, C. Gonzalez and J.A. Pople, Gaussian 94, Revision C.2, Gaussian Inc., Pittsburgh PA, 1995.
[27] J.M. Toussaint, F. Wudl, J.L. Brédas, J. Chem. Phys. 91 (1989) 1783–1788.
[28] J.J.P. Stewart, J. Comp. Chem. 10 (1989) 221–264.
[29] M.J.S. Dewar, R.J. Pettit, J. Chem. Soc. (1954) 1617; D. Peters, ibid. (1958) 1023.
[30] K. Yates, Hückel Molecular Orbital Theory, Academic, New York, 1978, p. 120.
[31] M. Saunders, R. Berger, A. Jaffe, J.M. McBride, J. O'Neill, R. Breslow, J.M. Hoffman, C. Perchonok Jr., E. Wasserman, R.S. Hutton, V.J. Kuck, J. Am. Chem. Soc. 95 (1973) 3017–3018.
[32] A. Nicolaides, D.M. Smith, F. Jensen, L. Radom, J. Am. Chem. Soc. 119 (1997) 8083–8088.
[33] J. Hrušák, D. Schröder, S. Iwata, J. Chem. Phys. 106 (1997) 7541–7549.
[34] S. Klippenstein, Int. J. Mass Spectrom. Ion Processes, 167/168 (1997) 235–257.
[35] I. Fleming, Frontier Orbitals and Organic Chemical Reactions, Wiley, New York, 1976.
[36] N.T. Anh, Orbitales Frontières, Manuel pratique, InterÉditions/CNRS Éditions, 1995.
[37] V. Le Page, V.M. Bierbaum, T.P. Snow, unpublished.
[38] T.P. Snow, V. Le Page, Y. Keheyan, V.M. Bierbaum, Nature (London) 391 (1998) 259–260.